

## II. 研究成果の刊行に関する一覧表

## II. 研究成果の刊行に関する一覧表

雑誌

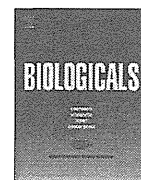
発表者氏名	論文タイトル名	発表誌名	巻号	ページ	出版年
Takayama-Ito M, Nakamichi K, Kinoshita H, Kakiuchi S, Kurane I, Saijo M, Lim CK.	A sensitive <i>in vitro</i> assay for the de tection of residual viable rabies virus in inactivated rab ies vaccines.	Biologicals	42	42 - 47	2014
Kuramitsu M, Okuma K, Yamagishi M, Yamochi T, Firouzi S, Momose H, Mizukami T, Takizawa K, Araki K, Sugamura K, Yamaguchi K, Watanabe T, Hamaguchi I.	Identification of TL-Om1, an Adult T-Cell Leukemia (ATL) Cell Line, as Reference Material for Quantitative PCR for Human T-Lymphotropic Virus 1.	J Clin Microbiol.	Vol.53 No.2	587 - 596	2015
Mizukami T, Momose H, Kuramitsu M, Takizawa K, Araki K, Furuhashi K, Ishii KJ, Hamaguchi I, Yamaguchi K.	System vaccinology for the evaluation of influenza vaccine safety by multiplex gene detection of novel biomarkers in a preclinical study and batch release test.	PLoS One.	Vol.9 Issue7	e1018 35.	2014
Kasama Y, Mizukami T, Kusunoki H, Peveling-Oberhag J, Nishito Y, Ozawa M, Kohara M, Mizuochi T, Tsukiyama-Kohara K.	B-cell-intrinsic hepatitis C virus expression leads to B-cell-lymphomage nesis and induction of NF- $\kappa$ B signalling.	PLoS One	Vol.9 Issue3	e9137 3	2014
多屋 馨子	副反応に対する 情報収集と 迅速な対応	チャイルド ヘルス	Vol.17 No.9	611 - 614	2014

発表者氏名	論文タイトル名	発表誌名	巻号	ページ	出版年
Takizawa K, Nakashima T, Mizukami T, Kuramitsu M, Endoh D, Kawauchi S, Sasaki K, Momose H, Kiba Y, Mizutani T, Furuta RA, Yamaguchi K, Hamaguchi I.	Degenerate polymerase chain reaction strategy with DNA microarray for detection of multiple and various subtypes of virus during blood screening.	Transfusion	53	2545 - 2555	2013
Odaka C, Kato H, Otsubo H, Takamoto S, Okada Y, Taneichi M, Okuma K, Sagawa K, Hoshi Y, Tasaki T, Fujii Y, Yonemura Y, Iwao N, Tanaka A, Okazaki H, Momose SY, Kitazawa J, Mori H, Matsushita A, Nomura H, Yasoshima H, Ohkusa Y, Yamaguchi K, Hamaguchi I.	Online reporting system for transfusion-related adverse events to enhance recipient haemovigilance in Japan: a pilot study.	Transfus Apher Sci.	48	95 - 102	2013
Krayukhina E, Uchiyama S, Nojima K, Okada Y, Hamaguchi I, Fukui K.	Aggregation analysis of pharmaceutical human immunoglobulin preparations using size-exclusion chromatography and analytical ultracentrifugation sedimentation velocity.	J Biosci Bioeng.	Vol.115 No.1	104 - 110	2013
Okajima K, Iseki K, Koyano S, Kato A, Azuma H.	Virological Analysis of a Regional Mumps Outbreak in the Northern Island of Japan—Mumps Virus Genotyping and Clinical Description.	Jpn. J. Infect. Dis	66(6)	561 - 563	2013

発表者氏名	論文タイトル名	発表誌名	巻号	ページ	出版年
Abe M, Tahara M, Sakai K, Yamaguchi H, Kanou K, Shirato K, Kawase M, Noda M, Kimura H, Matsuyama S, Fukuhara H, Mizuta K, Maenaka K, Ami Y, Esumi M, Kato A, Takeda M.	TMPRSS2 is an activating protease for respiratory parainfluenza viruses.	J Virol.	Vol.87 No.21	11930 - 11935	2013
Nagata S, Maedera T, Nagata N, Kidokoro M, Takeuchi K, Kuranaga M, Takeda M and Kato A.	Comparison of the live attenuated mumps vaccine (Miyahara strain) with its preattenuated parental strain.	J Vaccines Immun.	1(2)	13 - 21	2013
Wood D, Elmgren L, Li S, Wilson C, Ball R, Wang J, Cichutek K, Pfliederer M, Kato A, Cavaleri M, Southern J, Jivapaisarnpong T, Minor P, Griffiths E, and Sohn Y.	A Global Regulatory Science Agenda for Vaccines.	Vaccine	31	163 - 175	2013
多屋 馨子	副反応報告と 救済制度	公衆衛生	Vol.78 No.2	86 - 92	2014
Chikako Odaka, Hidefumi Kato, Hiroko Otsubo, Shigeru Takamoto, Yoshiaki Okada, Maiko Taneichi, Kazu Okuma, Kimitaka Sagawa, Yasutaka Hoshi, Tetsunori Tasaki, Yasuhiko Fujii, Yuji Yonemura, Noriaki Iwao, Asashi Tanaka, Hitoshi Okazaki, Shun-ya Momose, Junichi Kitazawa, Hiroshi Mori, Akio Matsushita, Hisako Nomura, Hitoshi Yasoshima, Yasushi Ohkusa, Kazunari Yamaguchi, Isao Hamaguchi,	Online reporting system for transfusion-related adverse events to enhance recipient haemovigilance in Japan: A pilot study	Transfusion and Apheresis Science	48	95 - 102	2013

発表者氏名	論文タイトル名	発表誌名	巻号	ページ	出版年
Shuetsu Fukushi, Mina Nakauchi, Tetsuya Mizutani, Masayuki Saijo, Ichiro Kurane, Shigeru Morikawa	Antigen-capture ELISA for the detection of Rift Valley fever virus nucleoprotein using new monoclonal antibodies	Journal of Virological Methods	180	68 - 74	2012
Kazunari Kondo, Asami Uenoyama, Ryo Kitagawa, Hajime Tsunoda, Rika Kusumoto-Matsuo, Seiichiro Mori, Yoshiyuki Ishii, Takamasa Takeuchi, Tadahito Kanda Iwao Kukimoto	Genotype Distribution of Human Papillomaviruses in Japanese Women with Abnormal Cervical Cytology	The Open Virology Journal	6, (Suppl 2: M14)	277 - 283	2012
内藤 誠之郎	ワクチン・レギュレ ーションの新展開 - 国家検定へのSLP 審査制度の 導入	PHARM TECH JAPAN	Vol.28 No.10	25 - 31	2012

### III. 研究成果の刊行物・別刷



## A sensitive *in vitro* assay for the detection of residual viable rabies virus in inactivated rabies vaccines



Mutsuyo Takayama-Ito\*, Kazuo Nakamichi, Hitomi Kinoshita, Satsuki Kakiuchi, Ichiro Kurane, Masayuki Saijo, Chang-Kweng Lim

Department of Virology 1, National Institute of Infectious Diseases, 1-23-1 Toyama, Shinjuku-ku, Tokyo 162-8640, Japan

### ARTICLE INFO

#### Article history:

Received 24 June 2013

Received in revised form

31 October 2013

Accepted 7 November 2013

#### Keywords:

Inactivated rabies vaccine

Inactivation test

Replacement

Vaccine quality control

### ABSTRACT

Rabies is a viral disease transmitted through bites from rabid animals and can be prevented by vaccines. Clinically used rabies vaccines are prepared from inactivated rabies viruses grown in cell cultures or embryonated eggs. In Japan and across the world, tests that confirm complete inactivation, such as the *in vivo* suckling mouse assay, in which suckling mice are intracerebrally inoculated with vaccine products, are required for quality control. In this study, we developed a novel cell-based immunofluorescence assay that does not require mice for testing rabies vaccine inactivation for human use. The sensitivity of this cell-based *in vitro* assay was 5.7 times that of the *in vivo* suckling mouse assay, with a detection limit of one focus forming units per ml of test sample. This newly developed *in vitro* assay may replace the established *in vivo* suckling mouse assay for confirming viral vaccine inactivation.

© 2013 The International Alliance for Biological Standardization. Published by Elsevier Ltd. All rights reserved.

### 1. Introduction

Rabies is a zoonotic viral disease of the central nervous system caused by rabies viruses that can infect almost every mammalian species. Upon presentation of symptoms of rabies infection, the mortality rate is 100%. It is estimated that approximately 55,000 patients die of rabies each year [1], and the World Health Organization (WHO) estimates that more than 15 million people worldwide receive annual post-exposure vaccinations to prevent disease progression.

Rabies is a viral disease that can be prevented using vaccines that in humans are used for pre- and post-exposure prophylaxis. Currently, rabies vaccines for human use are produced by cultivating rabies viruses in cell cultures or embryonated eggs and then inactivating them using phenol,  $\beta$ -propiolactone, N-tributylphosphate, or formalin. Inactivation is a crucial step in the manufacture of rabies vaccines, and two cases of inactivation failures have been reported. In Brazil, 18 people died of rabies caused by incomplete rabies virus inactivation [2]. In 2004, the Food and Drug Administration (FDA) identified the presence of non-inactivated rabies virus in a single product lot using an inactivation test before product release; subsequently, manufacturers recalled vaccine lots produced during the same period [3].

Inactivation tests that confirm the absence of residual infectious rabies virus are conducted in purified bulk samples and/or final products. In several countries, National Regulatory Authorities (NRAs) and manufacturers use the *in vivo* suckling mouse assay to test rabies vaccine inactivation [4–9]. In this procedure, 10 or more suckling or adult mice are intracerebrally inoculated with vaccine products and the appearance of rabies-associated symptoms is subsequently monitored for 21 days. If any mice die or show symptoms between days 4 and 21, brain samples are collected and tested for residual infectious rabies virus by detecting rabies virus antigens in the samples or by injecting brain samples into five additional mice. The Japanese Pharmacopoeia (JP) [7] and minimum requirements for biological products (MRBP) [8] require testing of purified bulk samples and final products using the *in vivo* suckling mouse assay. According to the Japanese MRBP [8], at least 30 suckling mice must be intracerebrally injected with 20  $\mu$ l vaccine product and observed for 21 days.

It has been suggested that a cell-based *in vitro* assay could be used instead of the suckling mouse assay to avoid the use of animals and to facilitate data replication [10,11]. Both WHO and the European Pharmacopoeia (EP) permit *in vitro* alternatives for testing rabies vaccine inactivation [4,12]. Moreover, the report and recommendation of the European Centre for Validation of Alternative Methods (ECVAM) workshop 48 state that “the test for residual live virus should be conducted on the bulk sample using cell cultures, and tests in mice and rabbits should be conducted as

\* Corresponding author. Tel.: +81 3 4582 2668; fax: +81 3 5285 2115.

E-mail address: [mutsuito@nih.go.jp](mailto:mutsuito@nih.go.jp) (M. Takayama-Ito).

finished product tests" [13]. Only one report published in German by Blum et al. [14] demonstrates the use of an immunofluorescence assay with the same detection limits as those of the mouse test. Therefore, in this study, we developed a novel sensitive *in vitro* assay for assessment of rabies vaccine inactivation.

## 2. Material and methods

### 2.1. Vaccine

The freeze-dried inactivated rabies vaccine used in this study was produced in Japan for human use, and was purchased from Kaketsuken (Kumamoto, Japan). According to the manufacturer's package insert, one reconstituted vaccine dose (1.0 ml) contains more than  $10^7$  LD<sub>50</sub> inactivated high egg passage (HEP)-Flury rabies virus strain and less than 0.2-mg gelatin as stabilizer. The potency of one dose is at least 2.5 IU of rabies antigen. The virus was propagated in primary chick embryo cell cultures and was subsequently inactivated by incubating with 0.02 volumes of beta-propiolactone at 37 °C for 60 min. The inactivated virus was concentrated by ultrafiltration, purified by ultracentrifugation, and then dispensed into individual vials and lyophilized [15]. Vaccine was resuspended in 1.0 ml of provided distilled water according to the package insert.

### 2.2. Virus

We used the HEP-Flury rabies virus vaccine strain originating from Japanese vaccine seed stock [16,17]. This strain is lethal to suckling mice, but not to adult mice when administered by intracerebral inoculation [18]. The working virus stock was prepared from infected Neuro-2a cells and stored at –80 °C until use. Viral titers were determined by titration in Neuro-2a cells as previously described [19]. The virus titer of the working stock was  $1.0 \times 10^8$  focus forming units (ffu)/ml.

### 2.3. Mice

One-day-old specific pathogen-free outbred ddY mice were purchased from Nippon SLC Inc. (Shizuoka, Japan). Eight suckling mice were placed in a cage with their untreated mother. All animal procedures were conducted in accordance with the guidelines of the National Institute of Infectious Diseases (NIID) in Japan. Symptoms in mice were observed every day, and mice were euthanized upon becoming moribund.

### 2.4. Cell cultures

Neuro-2a cells were kindly provided by Dr. Satoshi Inoue (National Institute of Infectious Diseases, Tokyo, Japan), and Baby Hamster Kidney (BHK-21) cells were kindly provided by Dr. Kinjiro Morimoto (Yasuda Women's University, Hiroshima, Japan). HEK-293 cells were purchased from RIKEN BioResource Center (Ibaraki, Japan). Neuro-2a and BHK-21 cells were grown in Dulbecco's modified Eagle's medium (D5796, D-MEM, Sigma–Aldrich, St. Louis, MO, USA) supplemented with 10% fetal bovine serum (FBS; Life Technologies, Carlsbad, CA, USA), 100-U/ml penicillin, and 100-µg/ml streptomycin (Life Technologies, Carlsbad, CA, USA). HEK-293 cells were grown in Eagle's minimum essential medium (M4655, E-MEM, Sigma–Aldrich, St. Louis, MO, USA) containing 10% FBS, 0.1-mM nonessential amino acids (Life Technologies, Carlsbad, CA, USA), 100-U/ml penicillin, and 100-µg/ml streptomycin. For virus inoculation, cells were cultured in medium containing 2% FBS or 0.2% bovine serum albumin (BSA; A2153, Sigma–Aldrich, St. Louis, MO, USA). Neuro-2a and BHK-21 cells were generally passaged twice per week at split ratios of 1:6 and 1:10, respectively. HEK-293

cells were passaged once per week with a split ratio of 1:8. Neuro-2a cells were seeded into 24- or 96-well culture plates (Techno Plastic Products AG, Trasadingen, Switzerland) at a density of  $6 \times 10^4$  cells/cm<sup>2</sup> one day before inoculation. BHK-21 and HEK-293 cells were seeded into 24-well plates at a density of  $1 \times 10^5$  cells/cm<sup>2</sup>. All cultures were incubated in a humidified incubator at 37 °C with 5.0% CO<sub>2</sub>, unless stated otherwise.

### 2.5. Direct immunofluorescent assays (DIFA)

In general, cells were cultured in 24- or 96-well culture plates for one day and then inoculated with diluted rabies virus. After 48–72 h, the culture medium was removed and allowed to dry in a safety cabinet for 10 min, and was then fixed in cold acetone for 20 min. After fixation, cells in culture plates were washed once with 0.01-M phosphate-buffered saline [PBS(–), Wako Pure Chemical Industries, Osaka, Japan] and stained with fluorescein isothiocyanate (FITC)-labeled anti-rabies mAb (Fujirebio Inc, Tokyo, Japan) for 40 min at 37 °C in a humidity chamber. Subsequently, cells in culture plates were washed 3 times in PBS(–) and culture plates were examined using a fluorescence microscope with an excitation filter BP460–490, dichroic mirror DM500, and barrier filter BA520IF (Olympus, Tokyo, Japan). Antigen-positive cells were identified as those containing small fluorescent cytoplasmic granules. All wells were screened in lines from top to bottom at 40× magnification, and rabies-specific fluorescent granules were confirmed at high magnification (200×). As positive and negative controls for DIFA, we used the HEP-Flury-infected or mock-infected Neuro-2a cells prepared on 12-well microscope slides (Iwaki, Tokyo, Japan).

### 2.6. *In vivo* suckling mouse assay

The *in vivo* suckling mouse assay was performed according to the Japanese MRBP [8]. Mice aged 4 days or younger were intracerebrally inoculated with 20-µl vaccine product. After inoculation, mice were monitored for 21 days for clinical symptoms and death. Mice deaths occurring within 4 days of inoculation were regarded as rabies unrelated death and were excluded from further analysis. Mice showing signs of rabies such as paralysis and convulsions at day 21 were included in analyses of rabies-related deaths.

## 3. Results

### 3.1. Selection of the most sensitive cell line

Sensitivities of Neuro-2a, BHK-21, and HEK-293 cells to rabies virus infection were determined. Neuro-2a and BHK-21 cells are commonly used in rabies studies, and HEK-293 cells are reportedly as sensitive as Neuro-2a cells in rapid rabies virus isolation experiments [20]. Confluent monolayers of BHK-21, Neuro-2a, and HEK-293 cells were cultured in 24-well plates and inoculated with 10-fold serial dilutions of the HEP-Flury strain in D-MEM containing 2% FBS (DMEM2). After 48 h incubation at 37 °C, cells were fixed and stained with FITC-labeled anti-rabies mAb as described above. Culture plates were observed under a fluorescent microscope at 200× magnification. The number of rabies antigen-positive foci did not differ between cell types, but foci in Neuro-2a cells were larger than those in BHK-21 and HEK-293 cells (Fig. 1). Thus, Neuro-2a cells were selected for further analyses.

### 3.2. Determination of optimal culture conditions

Neuro-2a cell culture conditions may influence virus-detection efficiencies. Accordingly, we analyzed the effects of incubation temperatures, culture medium supplements, and times of



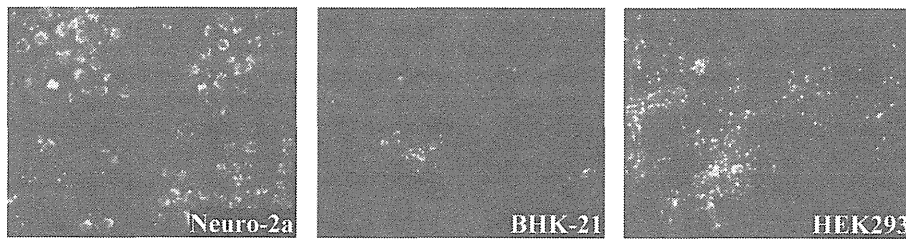


Fig. 1. Immunofluorescent signals of rabies virus antigens in cells infected with the HEP-Flury strain. Neuro-2a (left panel), BHK-21 (middle panel), and HEK-293 (right panel) were inoculated with the HEP-Flury rabies virus strain at a multiplicity of infection of 0.5 ffu. Original magnification, 200 $\times$ .

incubation. Neuro-2a cells in 96-well plates were inoculated with 10-times serially diluted virus (range 0–1000 ffu/well; 3 or 5 wells for each dose). Subsequently, cells were incubated with 100- $\mu$ l diluted virus suspensions and were assayed using DIFA as described above. Data from three independent experiments are shown in Fig. 2. Although detection rates at 35 °C were slightly higher than those at 37 °C (Fig. 2A), this difference was not statistically significant ( $p = 0.315$ ). Because the HEP-Flury strain is propagated in cells at 35 °C in vaccine production process, it is likely that low incubation temperatures slightly increased viral proliferation. Culture medium supplements (Fig. 2B) and time of incubation (Fig. 2C) did not affect residual virus detection rates. Consequently, in subsequent experiments, cells were cultured in DMEM2 at 35 °C for 72 h.

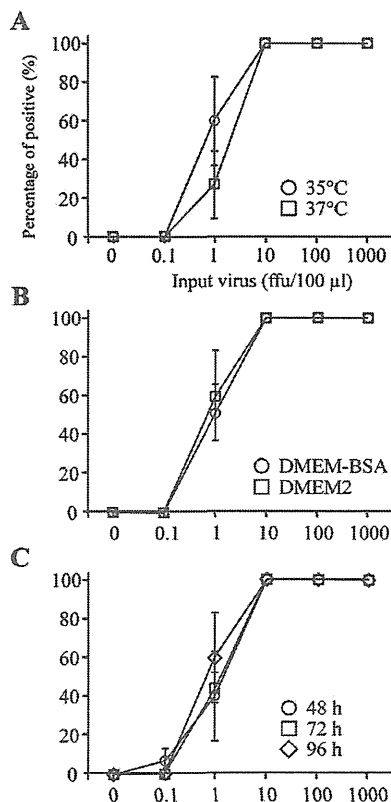


Fig. 2. Analysis of optimal culture conditions. Neuro-2a cells were cultured in 96-well plates and were inoculated with serial 10-fold dilutions of the HEP-Flury strain. Cells were incubated (A) for 72 h in DMEM2 at 35 °C or 37 °C, (B) for 72 h in DMEM containing 0.2% BSA or 2% FBS at 35 °C, or (C) for 48, 72, or 96 h in DMEM2 at 35 °C. After incubation, cells were fixed and viral antigen-positive cells were identified using DIFA.

### 3.3. Subculture of culture fluids increased the detectability of residual virus

Because additives and large quantities of inactivated virus particles in original inoculums may affect the infectivity of residual active viruses by inhibiting viral replication or occupying viral receptors, viral proliferation might be enhanced by subculturing culture fluids. Assay designs are shown in Fig. 3. In these experiments, 2-ml reconstituted vaccine product was spiked with 20 ffu of the HEP-Flury strain, and 10 ml of DMEM2 was then added. Neuro-2a cell medium was removed from 96-well plates. Mixtures of DMEM2 and vaccine containing virus were dispensed onto the plates and cells were incubated at 35 °C for 72 h (original culture). Then, 50- $\mu$ l aliquots of culture fluid were transferred onto Neuro-2a

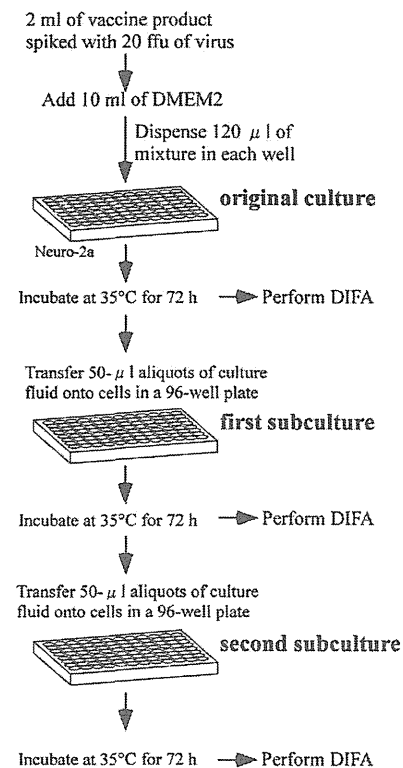


Fig. 3. Schematic of assay design for subculture of the culture fluid. Neuro-2a cells were cultured in 96-well plates and were inoculated with 2 ml of vaccine product spiked with 4 ffu of the HEP-Flury strain. After 72-h incubation, culture fluids were transferred onto newly prepared Neuro-2a cells and were incubated for a further 72 h. Culture fluids were then transferred again onto fresh Neuro-2a cells. After incubation, cells were fixed, and antigen-positive cells were identified using DIFA.

cells that were freshly seeded onto another 96-well plate. Culture plates inoculated with virus-spiked DMEM2 were fixed with acetone for DIFA. Subsequently, cells that were inoculated with original culture fluid were incubated for 72 h at 35 °C (first-subculture), and 50- $\mu$ l aliquots of culture fluid were transferred onto newly seeded Neuro-2a cells in 96-well plates. The plates that were inoculated with the original culture fluid were fixed as above. Plates inoculated with first subculture fluid were incubated for 72 h at 35 °C and were fixed (second subculture). Table 1 shows data from three independent experiments. The number of virus antigen-positive wells increased in subculture with culture fluid. The number of positive wells in the first-subculture was same as that in the second subculture. Hence, the first subculture was used for further analyses.

### 3.4. *In vitro* cell-based immunofluorescence assay

From the results above, we developed a novel *in vitro* cell-based immunofluorescent assay, in which 2 ml of reconstituted rabies vaccine is mixed with 10 ml of DMEM2 and is then dispensed onto Neuro-2a cells cultured in 96-well plates. Culture medium is then removed and 120- $\mu$ l aliquots of the mixture are dispensed per well. Cells are then incubated at 35 °C for 3 days, and 50- $\mu$ l aliquots of culture supernatant are transferred onto another 96-well plate containing fresh cells. Plates are used for DIFA after incubation for 72 h at 35 °C.

### 3.5. Comparison of sensitivity between *in vitro* and *in vivo* assays

Sensitivities of *in vivo* and *in vitro* assays were compared. As shown in Fig. 4, reconstituted vaccine products were spiked with the infectious HEP-Flury strain at doses of 150, 30, 6, 1.2, 0.24, and 0.048 ffu/20  $\mu$ l using serial 5-times dilutions of the reconstituted vaccine product. For *in vitro* assays (left), 2-ml doses of sample were mixed with 10 ml of DMEM2 and were distributed onto Neuro-2a cells in 96-well plates (120  $\mu$ l/well containing 20- $\mu$ l virus spiked vaccine product). For *in vivo* assays (right), each sample dose was inoculated into 8 suckling mice by intracerebral injection (20  $\mu$ l/mouse). Experiments were performed 3 times on separate occasions and data are presented as the mean in Fig. 5. Although detection frequencies were identical in *in vitro* and *in vivo* assays with 0.048 ffu/well or mouse, positive detection rates after doses of 0.24, 1.2, and 6 ffu/well or mouse were significantly higher in *in vitro* than *in vivo* assays. Median lethal dose (LD<sub>50</sub>) values in suckling mice and median cell culture infective dose (CCID<sub>50</sub>) values from *in vitro* assays were calculated using probit analyses [21,22] with the Bioassay Assist software (NIID, Japan), and indicated by 50% positive doses (Table 2). CCID<sub>50</sub> values in the *in vitro* assay were significantly lower than equivalent LD<sub>50</sub> values in the *in vivo* assay ( $p < 0.001$ ). Moreover, narrower 95% confidence intervals were produced in *in vitro* assays than *in vivo* assays, probably due to small numbers of mice. Average CCID<sub>50</sub> and LD<sub>50</sub> values in each assay were  $0.465 \pm 0.097$  and  $2.650 \pm 0.99$  ffu/well or mouse, respectively, suggesting that the *in vitro* assay is 5.7 times more sensitive than the *in vivo* assay.

**Table 1**

Effects of subcultures on detectability of residual virus.

Exp. No.	Number of positive wells/plate		
	Original culture	First subculture	Second subculture
1	8	11	11
2	7	11	11
3	5	10	10

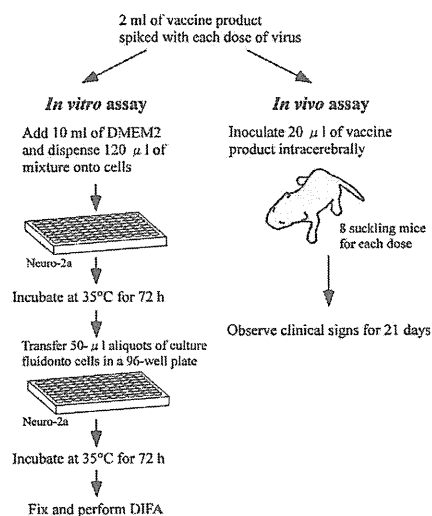


**Fig. 4.** Schematic of assay design for comparisons of *in vitro* and *in vivo* assays. The *in vitro* assay was performed using Neuro-2a cells cultured in 96-well plates. Reconstituted vaccine spiked with each dose of virus was mixed with the culture medium and added to Neuro-2a cells in 96-well plates. After 72 h incubation, 50- $\mu$ l aliquots of culture fluids were transferred onto fresh Neuro-2a cells on 96-well plates and further incubated for 72 h. The plates were tested for virus antigen using DIFA (left panel). The *in vivo* assay was performed in 8 suckling mice intracerebrally inoculated with vaccine suspensions. Clinical signs were observed for 21 days (right panel).

### 3.6. Detection limits of the *in vitro* assay

To determine the detection limits of the *in vitro* assay, we examined its sensitivity after spiking with very small quantities of virus in vaccine product. The HEP-Flury strain was spiked into the vaccine product at 0–0.125 ffu/well using serial 2-times dilutions of reconstituted vaccine product, and was inoculated into Neuro-2a cells in 96-well plates (Fig. 6). For each dose, 96 wells were inoculated. Only one positive well was detected at a dose of 0.008 ffu/well (Table 3). When 0.016 ffu of active virus was added per well (20  $\mu$ l), one or more positive wells were detected in 8 of 10 tests. The detection limit for the *in vitro* assay was 0.02 ffu/well, which was 3.3 times the SD of the regression line  $y$ -intercept and the slope of the low concentration curve according to the VICH Guideline 2

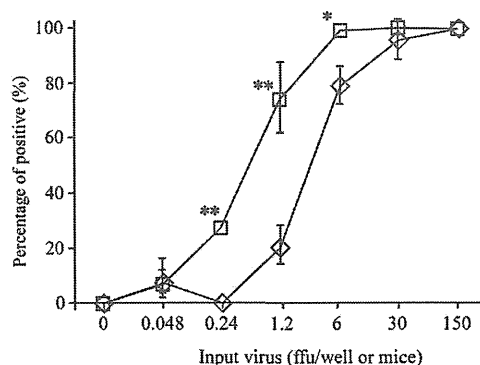


**Fig. 5.** Percentages of positive replicates in *in vitro* and *in vivo* assays. Percentage of positive wells in the *in vitro* assay was calculated as (number of positive wells/96)  $\times$  100 (open square) and that in the *in vivo* assay was calculated as (number of dead mice/8 suckling mice)  $\times$  100 (open rhombus). Data were expressed as the mean  $\pm$  SD of three independent experiments. Significant differences were identified using Student's  $t$ -test; \* $P < 0.05$ , \*\* $P < 0.01$ .

**Table 2**  
50% positive dose in *in vitro* and *in vivo* assays.

Exp. No.	Number of positive wells/plate	
	<i>In vitro</i> assay <sup>a</sup>	<i>In vivo</i> assay <sup>b</sup>
1	0.363 (0.295–0.447)	2.536 (0.949–6.852)
2	0.556 (0.434–0.707)	2.707 (1.241–5.881)
3	0.477 (0.388–0.589)	2.707 (1.241–5.877)

Each dose was tested *in vitro* and *in vivo* in 96 wells and 8 suckling mice, respectively.

<sup>a</sup> CCID<sub>50</sub> of *in vitro* assay: ffu/well (95% CI).

<sup>b</sup> LD<sub>50</sub> of *in vivo* assay: ffu/mouse (95% CI).

[23], and was equivalent to 1 ffu/ml of vaccine product. Virus input strongly correlated ( $r^2 = 0.96$ ) with numbers of positive wells.

#### 4. Discussion

Confirmation of inactivation and potency of rabies vaccines is necessary before release for human use. Because inactivation failure can cause death [2], vaccine inactivation test are crucial for vaccine quality assurance. In Japan and across the world, manufacturers are required to perform such testing after harvesting inactivated and final products according to the WHO TRS, the Japanese MRBP, and other regulatory authorities [4–8,12].

The WHO and EP allow NRAs and manufacturers to use *in vitro* cell-based assays for inactivation testing [4,12]. Mitchell et al. [24] developed a sensitive inactivation test for rabies vaccines. Although this assay still uses animals, the vaccine is passed through primary hamster kidney cell cultures before mouse inoculation. Using this combination method, the virus is detected with at least 100 times more sensitivity than direct mouse inoculation methods. Because they used immunocompetent adult mice for mouse inoculation test, this significant enhancement may reflect immunological effects. Equivalent sensitivity of cell-based and *in vivo* assays for residual infectious West Nile virus [25] has been reported, suggesting that cell-based methods are equally or more sensitive than suckling mouse inoculation methods. Furthermore, implementation of intracerebral inoculation requires extensive training and skills; in addition, accidental death of suckling mice occurs in approximately 9% cases in our laboratory. However, animal-based rabies inactivation tests before batch release are still used by manufacturers and NRAs in several countries, including Japan, partly because no practical *in vitro* inactivation test is available for rabies vaccines. Although an excellent report was published by Blum et al. [14], the article is available only in German. Nonetheless,

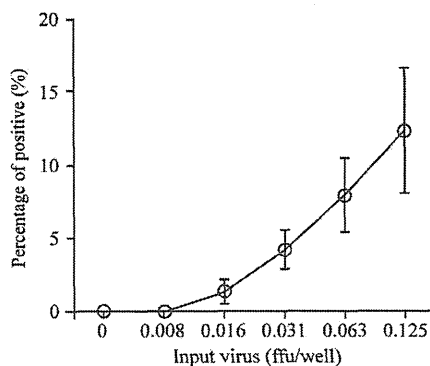


**Fig. 6.** Percentages of positive wells in the *in vitro* assay at very low doses. Percentages of positive wells in very low-dose the *in vitro* assays were calculated as shown in Fig. 5. Data are presented as the mean  $\pm$  SD from 10 independent experiments.

**Table 3**  
Number of positive wells in *in vitro* assay at very low doses.

Exp.No.	Input virus (ffu/well)					y-Intercept <sup>a</sup>	Slope <sup>b</sup>	DL <sup>c</sup>
	0.008	0.016	0.031	0.063	0.125			
1	0	2	2	4	9	-0.04	71	0.029
2	0	2	6	11	21	-0.50	175	0.012
3	0	2	5	9	9	1.46	73	0.028
4	0	1	4	6	8	0.63	66	0.031
5	1	2	6	11	16	0.96	129	0.016
6	0	0	3	5	10	-0.58	86	0.024
7	0	2	4	9	14	0.13	117	0.017
8	0	2	5	5	12	0.33	92	0.022
9	0	1	3	9	12	0.29	89	0.023
10	0	0	3	7	7	0.29	64	0.032
Average	0.1	1.4	4.1	7.6	11.8	0.30	96	0.023

<sup>a</sup> y-Intercept of the linear regression.

<sup>b</sup> Slope of the linear regression.

<sup>c</sup> Detection limit was calculated as  $3.3 \times$  SD of y-intercepts/slope.

summaries of their protocols appear in WHO TRS [12] and EP monographs [4]. In particular, the WHO TRS method involves cell adsorption of the vaccine, trypsinization on day 7, and observation of cultures for at least 21 days [12]. The protocol in EP monographs is similar to that in the WHO TRS, but the observation period is 14 days [4]. These methods require large volumes of cultured cells and take over 14 days for completion. In the present study, we developed a new *in vitro* assay for the confirmation of rabies virus inactivation.

The WHO recommends tests to be conducted on those cell lines that are used for production or on others that have demonstrated greater sensitivity in inactivation tests [12]. Primary chick embryo cells, which are used for production of the rabies vaccine in Japan, were not examined in this study because primary cell cultures are more complicated to use than immortalized cell lines and are considered unfavorable for constant use in tests of inactivation. Nonetheless, purified Vero cell vaccine (PVRV) and human diploid cell vaccine (HDRV) must be examined using Vero cells and human diploid cells, respectively. In the present study, subculture of supernatants from inoculated cells enhanced residual virus detection efficiency and was easier to perform than the reported cell trypsinization methods [4,12,26].

Sensitivity was significantly higher in the present *in vitro* assay than in the *in vivo* assay, and provides a novel inactivation test for rabies vaccines with sufficient reliability to be licensed as a standard assay. Small mouse numbers (8 suckling mice/dose) potentially lead to comparative insensitivity of the *in vivo* assay. Indeed, the probability of infection in the *in vitro* assay is heightened by an increased number of replicates, and positive detection was observed at a dose of 0.048 ffu/well or mouse. Increasing mice numbers are not practical; thus, giving rise to a significant advantage of the *in vitro* approach. A large number of samples also contributed to the high precision of the *in vitro* assay.

In this study, we showed detection limits as 10 times lower than those previously reported [14]. This increased sensitivity may reflect cell types (Neuro-2a or BHK-21), virus strains (HEP-Flury or CVS), incubation conditions, or other differences. In the previous study, BHK-21 cells were cultured in 96-well micro titer plates and were inoculated with 30- $\mu$ l samples of the CVS rabies virus strain in 100  $\mu$ l of MEM without FBS. After 2 days incubation at 34  $^{\circ}$ C, cells were fixed and immunofluorescence assays were performed using anti-Rabies G protein-FITC-conjugated antibodies. In agreement with the present data, the previous study showed no inhibition of active virus, even in the presence of high concentrations of inactivated virus. Although adjuvants and preservatives reportedly affect *in vitro* test detection limits, we did not verify this in direct comparisons of the present vaccine and preservative-free test samples.

The present *in vitro* assay takes only 6 days to perform, whereas current suckling mouse inoculation methods require 14–21 days [4–8,12]. In addition to improvements in animal welfare, the *in vitro* assay is easier, more cost-effective, and less time-consuming than the established *in vivo* assay that is performed according to Japanese MRBP [8], EP monographs [4], and WHO technical reports [12].

In summary, we developed a novel *in vitro* assay and confirmed its sensitivity in comparison to the *in vivo* suckling mouse assay. Although further validation of each vaccine product is required to investigate the influences of adjuvants and other additives, the present *in vitro* assay may be a useful method for testing of both human and veterinary vaccines. The present data warrant further consideration of this *in vitro* assay for routine quality assurance of inactivated rabies vaccines.

#### Acknowledgments

All animal studies were performed in accordance with the Research Animal Care Policies of the NIID (approval code H23-110068). This work was supported by JSPS KAKENHI, Grant Number 23790516, and a Grant in Aid from the Ministry of Health Labour and Welfare, Japan; Grant Numbers H21-IYAKU-IPPAN-010 and H24-IYAKU-IPPAN-002. The authors would like to thank Enago ([www.enago.jp](http://www.enago.jp)) for the English language review.

#### References

- [1] Knobel DL, Cleaveland S, Coleman PG, Fèvre EM, Meltzer MI, Miranda MEG, et al. Re-evaluating the burden of rabies in Africa and Asia. *Bull World Health Organ* 2005;83:360–8.
- [2] Pará M. An outbreak of post-vaccinal rabies (rage de laboratoire) in Fortaleza, Brazil, in 1960. Residual fixed virus as the etiological agent. *Bull World Health Organ* 1965;33:177–82.
- [3] CDC. Notice to Readers: manufacturer's recall of human rabies vaccine. *Morb Mortal Wkly Rep* 2004;53:287–9.
- [4] European Pharmacopoeia. Rabies vaccine for human use prepared in cell cultures. In: Monograph 0216 2008. pp. 699–701.
- [5] U.S. Pharmacopoeia. Rabies vaccine. USP29-NF24; 2012. p. 1887.
- [6] British Pharmacopoeia. Rabies veterinary vaccine, inactivated. In: Monograph 0451 2012.
- [7] The Japanese Pharmacopoeia. Freeze-dried inactivated tissue culture rabies vaccine: in official monographs. 16th ed.; 2011. p. 1333.
- [8] National Institute of Infectious Diseases. Freeze-dried inactivated tissue culture rabies vaccine. In: Minimum requirements for biological products 2006. pp. 40–3.
- [9] Gifford G, Agrawal P, Hutchings D, Yarosh O. Veterinary vaccine post-licensing safety testing: overview of current regulatory requirements and accepted alternatives. *Procedia Vaccinol* 2011;5:236–47.
- [10] Stokes W, Kulpa-Eddy J, McFarland R. The international workshop on alternative methods to reduce, refine, and replace the use of animals in vaccine potency and safety testing: introduction and summary. *Procedia Vaccinol* 2011;5:1–15.
- [11] Kulpa-Eddy J, Srinivas G, Halder M, Brown K, Draayer H, Galvin J, et al. Alternative methods and strategies to reduce, refine, and replace animal use for veterinary vaccine post-licensing safety testing: state of the science and future directions. *Procedia Vaccinol* 2011;5:106–19.
- [12] World Health Organization. Annex 2 Recommendations for inactivated rabies vaccine for human use produced in cell substrates and embryonated eggs. In: WHO Expert Committee on biological Standardization, Fifty-sixth report, technical report Series. vol. 941; 2007. pp. 83–132.
- [13] Bruckner L, Cussler K, Halder M, Baratt J, Castle P, Duchow K, et al. Three Rs approaches in the quality control of inactivated rabies vaccines. *Altern Lab Anim* 2003;31:429–54.
- [14] Blum SA, Braunschweiger M, Krämer B. How to prove complete virus inactivation in rabies vaccines. A comparison of an *in vivo* to an *in vitro* method. *Altex* 1998;15:46–9.
- [15] Yamada A, Kuniaki S, Sako M, Nonaka S. Production and quality control of rabies vaccine. In: Fukai K, editor. Virus vaccines in Asian countries. Tokyo: University of Tokyo Press; 1986. pp. 83–90.
- [16] Kondo A. Growth characteristics of rabies virus in primary chick embryo cells. *Virology* 1965;27:199–204.
- [17] Arai YT, Ogata T, Oya A. Studies on Japanese-produced chick embryo cell culture rabies vaccines. *Am J Trop Med Hyg* 1991;44:131–4.
- [18] Koprowski H, Black J. Studies on chick-embryo adapted rabies virus. II. Pathogenicity for dogs and use of egg-adapted strains for vaccination purposes. *J Immunol* 1950;64:185–96.
- [19] Inoue KI, Shoji Y, Kurane I, Iijima T, Sakai T, Morimoto K. An improved method for recovering rabies virus from cloned cDNA. *J Virol Methods* 2003;107:229–36.
- [20] Madhusudana SN, Sundaramoorthy S, Ullas PT. Utility of human embryonic kidney cell line HEK-293 for rapid isolation of fixed and street rabies viruses: comparison with Neuro-2a and BHK-21 cell lines. *Int J Infect Dis* 2010;14:1067–71.
- [21] Bliss CI. The calculation of the dosage-mortality curve. *Ann Appl Biol* 1935;22:134–67.
- [22] Bliss CI. The determination of the dosage-mortality curve from small numbers. *Quart J Pharm Pharmacol* 1938;11:192–216.
- [23] Validation of analytical procedures: methodology. Implemented in October 1999. Available at: [http://www.vichsec.org/pdf/g102\\_st7.pdf](http://www.vichsec.org/pdf/g102_st7.pdf).
- [24] Mitchell JR, Everest RE, Anderson GR, Control D. Sensitive procedure for detecting residual viable virus in inactivated rabies vaccine. *Appl Microbiol* 1971;22:600–3.
- [25] Koldijk MH, Bogaards JA, Kostense S, de Vocht M, Gijssbers L, Ter Haak M, et al. A sensitive cell-based assay for the detection of residual infectious West Nile virus. *Vaccine* 2007;25:6872–81.
- [26] Mondal SK, Neelima M, Reddy KSR, Rao KA, Srinivasan VA. Validation of the inactivant binary ethylenimine for inactivating rabies virus for veterinary rabies vaccine production. *Biologicals* 2005;33:185–9.

# Identification of TL-Om1, an Adult T-Cell Leukemia (ATL) Cell Line, as Reference Material for Quantitative PCR for Human T-Lymphotropic Virus 1

Madoka Kuramitsu,<sup>a</sup> Kazu Okuma,<sup>a</sup> Makoto Yamagishi,<sup>b</sup> Tadanori Yamochi,<sup>b</sup> Sanaz Firouzi,<sup>b</sup> Haruka Momose,<sup>a</sup> Takuo Mizukami,<sup>a</sup> Kazuya Takizawa,<sup>a</sup> Kumiko Araki,<sup>a</sup> Kazuo Sugamura,<sup>c</sup> Kazunari Yamaguchi,<sup>a</sup> Toshiki Watanabe,<sup>b</sup> Isao Hamaguchi<sup>a</sup>

Department of Safety Research on Blood and Biological Products, National Institute of Infectious Diseases, Tokyo, Japan<sup>a</sup>; Department of Medical Genome Sciences, Laboratory of Tumor Cell Biology, Graduate School of Frontier Sciences, The University of Tokyo, Tokyo, Japan<sup>b</sup>; Division of Molecular and Cellular Oncology, Miyagi Cancer Center Research Institute, Natori, Japan<sup>c</sup>

Quantitative PCR (qPCR) for human T-lymphotropic virus 1 (HTLV-1) is useful for measuring the amount of integrated HTLV-1 proviral DNA in peripheral blood mononuclear cells. Many laboratories in Japan have developed different HTLV-1 qPCR methods. However, when six independent laboratories analyzed the proviral load of the same samples, there was a 5-fold difference in their results. To standardize HTLV-1 qPCR, preparation of a well-defined reference material is needed. We analyzed the integrated HTLV-1 genome and the internal control (IC) genes of TL-Om1, a cell line derived from adult T-cell leukemia, to confirm its suitability as a reference material for HTLV-1 qPCR. Fluorescent *in situ* hybridization (FISH) showed that HTLV-1 provirus was monoclonally integrated in chromosome 1 at the site of 1p13 in the TL-Om1 genome. HTLV-1 proviral genome was not transferred from TL-Om1 to an uninfected T-cell line, suggesting that the HTLV-1 proviral copy number in TL-Om1 cells is stable. To determine the copy number of HTLV-1 provirus and IC genes in TL-Om1 cells, we used FISH, digital PCR, and qPCR. HTLV-1 copy numbers obtained by these three methods were similar, suggesting that their results were accurate. Also, the ratio of the copy number of HTLV-1 provirus to one of the IC genes, RNase P, was consistent for all three methods. These findings indicate that TL-Om1 cells are an appropriate reference material for HTLV-1 qPCR.

Human T-lymphotropic virus 1 (HTLV-1) was the first retrovirus to be found in humans (1, 2). HTLV-1 is a cause of adult T-cell leukemia (ATL), HTLV-1-associated myelopathy/tropical spastic paraparesis (HAM/TSP), and HTLV-1-associated uveitis (3). Areas where HTLV-1 is endemic are distributed across several different regions, including southern Japan, the Caribbean, South America, and tropical Africa (4, 5). A recent report has shown that the area affected by this infection has expanded from the southern part of Japan to the entire country, particularly the Tokyo metropolitan area (6). Diagnostic tests for HTLV-1 infection are performed mainly with serological assays, such as enzyme-linked immunosorbent assay, particle agglutination assay, and Western blotting. Recently, another diagnostic test has been developed. Quantitation of integrated proviral DNA in peripheral blood (proviral load [PVL]) can be performed by quantitative PCR (qPCR) as a risk assessment for ATL or HAM/TSP (7, 8).

A few studies reported that several samples were positive for viral DNA when tested by PCR even though those samples had been found seroindeterminate for HTLV-1 when tested by Western blotting (9, 10). Their results suggest that HTLV-1 qPCR could be used as an additional test to confirm infection in seroindeterminate samples.

Although many laboratories have developed qPCR methods for HTLV-1 detection in Japan, a wide variety of testing methods are used. For example, the target region, primers and probes, and internal control (IC) genes vary among the laboratories (8, 11–15). These variations lead to significant differences in HTLV-1 PVL when these laboratories measure the same samples (16). As a consequence of these differences, comparison of quantitative data between laboratories will continue to be difficult without standardization.

One possible solution is to establish a reference material, which is indispensable for standardizing multicenter test results. The target material for HTLV-1 qPCR is genomic DNA (gDNA) from peripheral blood mononuclear cells (PBMCs). Therefore, HTLV-1-infected cells would be an ideal source for a reference material. To date, many cell lines from ATL patients have been established, but few of them have been well characterized for the genomic features associated with reference materials for HTLV-1 qPCR.

In this study, we investigated the genomic structure of one of these ATL cell lines, TL-Om1, to establish it as a reference material for HTLV-1 nucleic acid amplification techniques (NATs), namely, HTLV-1 clonality, karyotyping, proviral sequencing, integration sites, and determination of gene copy number of HTLV-1 and cellular genes for IC.

Received 5 August 2014 · Returned for modification 23 September 2014

Accepted 5 December 2014

Accepted manuscript posted online 10 December 2014

Citation Kuramitsu M, Okuma K, Yamagishi M, Yamochi T, Firouzi S, Momose H, Mizukami T, Takizawa K, Araki K, Sugamura K, Yamaguchi K, Watanabe T, Hamaguchi I. 2015. Identification of TL-Om1, an adult T-cell leukemia (ATL) cell line, as reference material for quantitative PCR for human T-lymphotropic virus 1. *J Clin Microbiol* 53:587–596. doi:10.1128/JCM.02254-14.

Editor: A. M. Callendo

Address correspondence to Isao Hamaguchi, i30hama@niid.go.jp.

Supplemental material for this article may be found at <http://dx.doi.org/10.1128/JCM.02254-14>.

Copyright © 2015, American Society for Microbiology. All Rights Reserved. doi:10.1128/JCM.02254-14

TABLE 1 Primers used for qPCR of HTLV-1 and IC genes

Target gene	Forward name	Forward sequence	Reverse name	Reverse sequence	Size (bp)	Primer correction factor	
						Plasmid	gDNA
HTLV-1 gene	LTR202F	ACAATGACCATGAGCCCCAAA	LTR202R	TTAGTCTGGGCCCTGACCT	101	0.9869	
	LTR215F	GCTCGCATCTCTCCTTAC	LTR215R	AGTTCAGGAGGCACCACA	102	0.9942	
	LTR005F	CCTGACCCTGCTTGCTCAAC	LTR005R	TCAGTCGTGAATGAAAGGGAAAG	99	0.9917	
	056F	TAGTCCCACCCTGTTCGAAATG	056R	GCCAGGAGAATGTCATCCATGT	105	1.0013	
	084F	CCTGCCCGCTTACTATCG	084R	GGCATCTGTGAGAGCGTTGA	102	0.9922	
	153F	TTGTGCGGCTACTCCTTCTTG	153R	AGGGATGACTCAGGGTTTATAAGAGA	118	0.9792	
	pX2-S <sup>a</sup>	CGGATACCCAGTCTACGTGT	pX2-AS <sup>a</sup>	CAGTAGGGCGTGACGATGTA	100	0.9944	
RNaseP (RPPH1) gene	RPPH1-05F	TATGCACAATTATGTAATCCCCAAA	RPPH1-05R	CCAGCTCCCTATAACCTGCACTT	100	1.0025	1.0012
	RPPH1-08F	GCCGGAGCTTGGAAACAGA	RPPH1-08R	AATGGGCGGAGGAGAGTAGTCT	109	0.9956	0.9937
	RPPH1-12F	AGGAAGCCCACGAAAATTCTAATT	RPPH1-12R	GTCCCCATACTCGGTGATTCTC	101	1.0019	1.0052
Albumin (ALB) gene	ALB-07F	TGCAATGAACACAGGAGACTACTA	ALB-07R	CCACCCAGGTAACAAAATTAGCAT	103	0.9971	0.9964
	ALB-19F	CCTGATGCTTCTCAGCCTGTT	ALB-19R	TCCATTTAAGAGTGTGTGGTAGGT	100	1.0019	1.0045
	ALB-26F	TGCATTGCCGAAGTGAAAA	ALB-26R	CCTCAGCATAGTTTTTGGCAAACA	100	1.0038	1.0078
β-Actin (ACTB) gene	ACTB-06F	TCTGGTGTGTTGTCTCTGACTAGGT	ACTB-06R	CCGCTTTACACCAGCCTCAT	100		0.9965
	ACTB-12F	TCCTGGGTGAGTGGAGACTGT	ACTB-12R	CCATGCCTGAGAGGGAAAATG	107		1.0016
	ACTB-21F	AGCATCCCCAAAGTTCACA	ACTB-21R	GGACTTCCTGTAACAACGCATCT	101		1.0106
CD81 gene	CD81-01F	GACACATCCCAAGGTGCTT	CD81-01R	GGACTCAGTTCTCAATGCTTTGC	107		1.0015
	CD81-10F	ACCACGCCTTGCCCTTCT	CD81-10R	GAATCACGCCACTTCCATAACTG	111		1.0021
	CD81-21F	GGTGCACACAGCATGCATTT	CD81-21R	GTGCGCCTCTGGGTAATCAT	102		1.0009
β-Globin (HBB) gene	HBB-11F	TTGGACCCAGAGTTCTTTGAG	HBB-11R	GGCACCGAGCACTTTCTTG	103		1.0021
	HBB-15F	AGCAGCTACAATCCAGCTACCAT	HBB-15R	GAGGTATGAACATGATTAGCAAAAGG	105		1.0033
	HBB-24F	CCCACCCCAATGGAAGTC	HBB-24R	AGCACCATAAGGGACATGATAAGG	104		1.0111
RAG-1 gene	RAG1-03F	GCAATCCCATTGTCCACTTTT	RAG1-03R	TCCCCTGGCCTGCATTACTA	100		1.0045
	RAG1-27F	GAAGTTTAGCAGTGCCCATGT	RAG1-27R	ACGGGCAGTGTTCAGATG	100		1.0006
	RAG1-32F	TCAAAGTCATGGCAGCTATTGT	RAG1-32R	AGGGAATTCAAGACGCTCAGAA	100		0.9993

<sup>a</sup> Primer sequences were previously reported in reference 11.

## MATERIALS AND METHODS

**Cells and gDNA preparation.** Jurkat clone E6-1 cells were obtained from the American Type Culture Collection. HUT102 and SLB-1 cells, which are HTLV-1-infected cell lines, were a kind gift from Masahiro Fujii (Division of Virology, Niigata University Graduate School of Medical and Dental Sciences). PBMCs were kindly provided by the Japanese Red Cross or purchased from AllCells (Alameda, CA, USA). TL-Om1 cells, an ATL-derived cell line established by Sugamura et al. (17), were maintained in RPMI 1640 (Sigma, St. Louis, MO, USA) containing 10% fetal bovine serum (FBS) supplemented with 100 U/ml penicillin-streptomycin (Invitrogen, Carlsbad, CA, USA), 2 mmol/liter L-glutamine, and 10 ng/ml interleukin-2 (PeproTech, London, United Kingdom). Jurkat, HUT102, and SLB-1 cells were maintained in RPMI 1640 containing 10% FBS supplemented with 100 U/ml penicillin-streptomycin and 2 mmol/liter L-glutamine. DNA was extracted using a QIAamp DNA blood mini or maxi kit (Qiagen, Valencia, CA, USA).

**Southern blotting.** Southern blotting was performed by SRL Inc. (Tokyo, Japan). DNA was digested with EcoRI and PstI and separated on a 0.8% agarose gel as previously reported (18, 19). DNA was transferred onto nylon membranes (Roche, Mannheim, Germany). The membrane was hybridized with digoxigenin (DIG)-labeled HTLV-1 probe at 42°C overnight. DNA fragments for HTLV-1 probes were obtained from Oncor Inc. (Gaithersburg, MD, USA). Sense and antisense HTLV-1 DNA probes were prepared by random primed labeling using a DIG-High Prime kit (Roche). After the membrane was washed, HTLV-1 probe signals were obtained using a DIG luminescent detection kit (Roche).

**FISH analysis.** To stop the cell cycle at M phase, Colcemid (Sigma) was added to the cell culture medium at a concentration of 0.02 µg/ml and incubated for 1 h. Cells were harvested and washed with phosphate-buffered saline (PBS). After treatment with 0.075 M KCl hypotonic solution at 37°C for 1 h, cells were fixed with a solution containing acetic acid and methanol (3:1). Cells were fixed to a glass slide and dried. The complete HTLV-1 genome inserted in pUC18 (15) was used as a probe for provirus, bacterial artificial chromosome (BAC) clone RP11-919G18 was used as a probe for the albumin (ALB) gene, and BAC clones CTD-2326H15 and RP11-203M5 were used as probes for the RNase P (RPPH1) gene. BAC clones were selected from NCBI (<http://www.ncbi.nlm.nih.gov/clone/>) and were purchased from Advanced Geno Techs Co. (Tsukuba, Japan). The probe for Iq44 was commercially prepared by Chromosome Science Labo Inc. (Sapporo, Japan). For the detection of ALB and RPPH1 genes, the BAC clones were labeled with cyanine 3 (Cy3) and Cy5, respectively. For the detection of provirus, the DIG-labeled probe was prepared by the nick translation method. The probe was hybridized to the sample at 70°C for 5 min, followed by incubation at 37°C overnight. The probe was stained with anti-DIG-Cy3 antibody. Signals were detected by a Leica DMRA2 system and analyzed with Leica CW4000 fluorescent *in situ* hybridization (FISH) software (Wetzlar, Germany).

**Splinkerette PCR analysis.** Splinkerette PCR was performed as previously reported (20). The first-round PCR was performed as indicated in reference 20. The second-round, nested PCR was performed using the HTLV-1 long-terminal-repeat (LTR)-specific primer. The nested PCR product was loaded onto 3% Tris-acetate-EDTA buffer (TAE) agarose gels. Two distinct DNA bands were cut from the agarose gel and purified using a QIAquick gel extraction kit (Qiagen). After thymine and adenine (TA) cloning, each band was sequenced by the Sanger method (21).

**Inverse PCR analysis.** TL-Om1 gDNA was digested with BamHI or XbaI. Digested DNA was purified by phenol-chloroform extraction followed by ethanol precipitation. Briefly, 1/10 volume of 3 M sodium acetate and 2.5 volume of 100% ethanol were added to the sample. After centrifugation at  $2 \times 10^4 \times g$  for 15 min, the DNA pellet was washed with 70% ethanol and then air dried. Purified DNA was self-ligated using a Ligation-Convenience kit (Nippon Gene, Tokyo, Japan). Ligated DNA was purified again by phenol-chloroform extraction followed by ethanol precipitation. PCR was performed with KOD FX (Toyobo, Osaka, Japan). The PCR mixture contained 20 ng gDNA, 0.4 mM forward and reverse

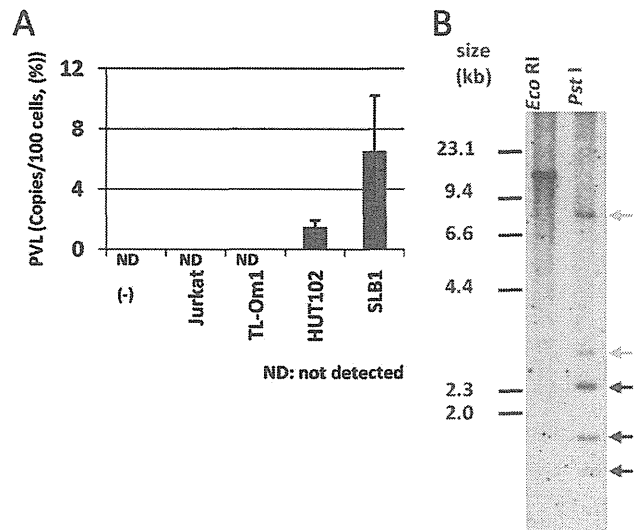


**FIG 1** Infectivity and clonality of HTLV-1 provirus in TL-Om1 cells. (A) Mitomycin C-treated Jurkat, TL-Om1, HUT102, and SLB1 cells were cocultured with Jurkat cells. PVL (%) was measured 2 weeks later by qPCR. (B) gDNA from TL-Om1 cells digested with EcoRI or PstI was subjected to Southern blotting probed by the full HTLV-1 genome. Three black arrows show bands for typical HTLV-1 genomic sequences; two gray arrows show bands for host genomic sequences ligated to the HTLV-1 genome. Because the EcoRI site is not included in the HTLV-1 sequence, the number of bands indicates the number of clones in the cells. Detection of two gray bands indicates that there is a pair of 5' and 3' HTLV-1 genomes conjugated with the host genome, signifying that the HTLV-1 provirus is monoclonal. On the other hand, detection of more than two gray bands indicates that it is multiclonal.

primers, 1 mM deoxynucleoside triphosphate (dNTP),  $1 \times$  KOD FX buffer, and 0.5 U KOD FX in a total volume of 25 µl, in duplicate. The forward primer sequence was 5'-ACAAATACACCTTGCATCCTATG G-3', and the reverse primer sequence was 5'-CGCTTGGGAGACTTCT TGCT-3'. PCR mixtures were denatured at 94°C for 2 min, followed by 34 cycles of 98°C for 10 s and 68°C for 10 min. PCR products were loaded onto 0.8% agarose gels and detected by LAS-3000 (Fujifilm, Tokyo, Japan).

**Genomic long PCR.** Genomic long PCRs were performed using KOD FX (Toyobo). Primers are listed in Table S1 in the supplemental material. The conditions for the PCR mixture and thermal cycling program were the same as those for the inverse PCR analysis.

**DNA sequencing analysis.** The genomic long PCR and inverse PCR products were purified by a GenElute PCR Clean Up kit (Sigma). Direct sequencing was performed using a BigDye Terminator v3.1 sequencing kit (Applied Biosystems, Foster City, CA, USA). Sequence primers are listed in Table S2 in the supplemental material. Sequences were read and analyzed using a 3120× genetic analyzer (Applied Biosystems).

**Synchronized qPCR analysis.** The primers used for the synchronized qPCR amplification are listed in Table 1. The PCR mixture was prepared with SYBR premix *Ex Taq* II (TaKaRa, Tokyo, Japan) containing 100 ng gDNA and 0.4 mM forward and reverse primers in a total volume of 15 µl, in triplicate. PCR was performed according to the manufacturer's protocol. The  $\Delta C_T(RPPH1)$  value (where  $C_T$  is threshold cycle) was calculated by the following equation:  $\Delta C_T(RPPH1) = \text{average } C_T \text{ of target gene primer results} - \text{average } C_T \text{ of RPPH1}$ . The gene copy number was calculated by the following equation:  $\text{target gene copy number } (N) = \text{copy number determined by FISH} \times 2^{-\Delta C_T(RPPH1)}$ . Using normal PBMCs or plasmids, the primer correction factor, which can compensate for small differences in amplification efficiency among different primers, was calculated. The correction factor was determined by the difference of each  $C_T$

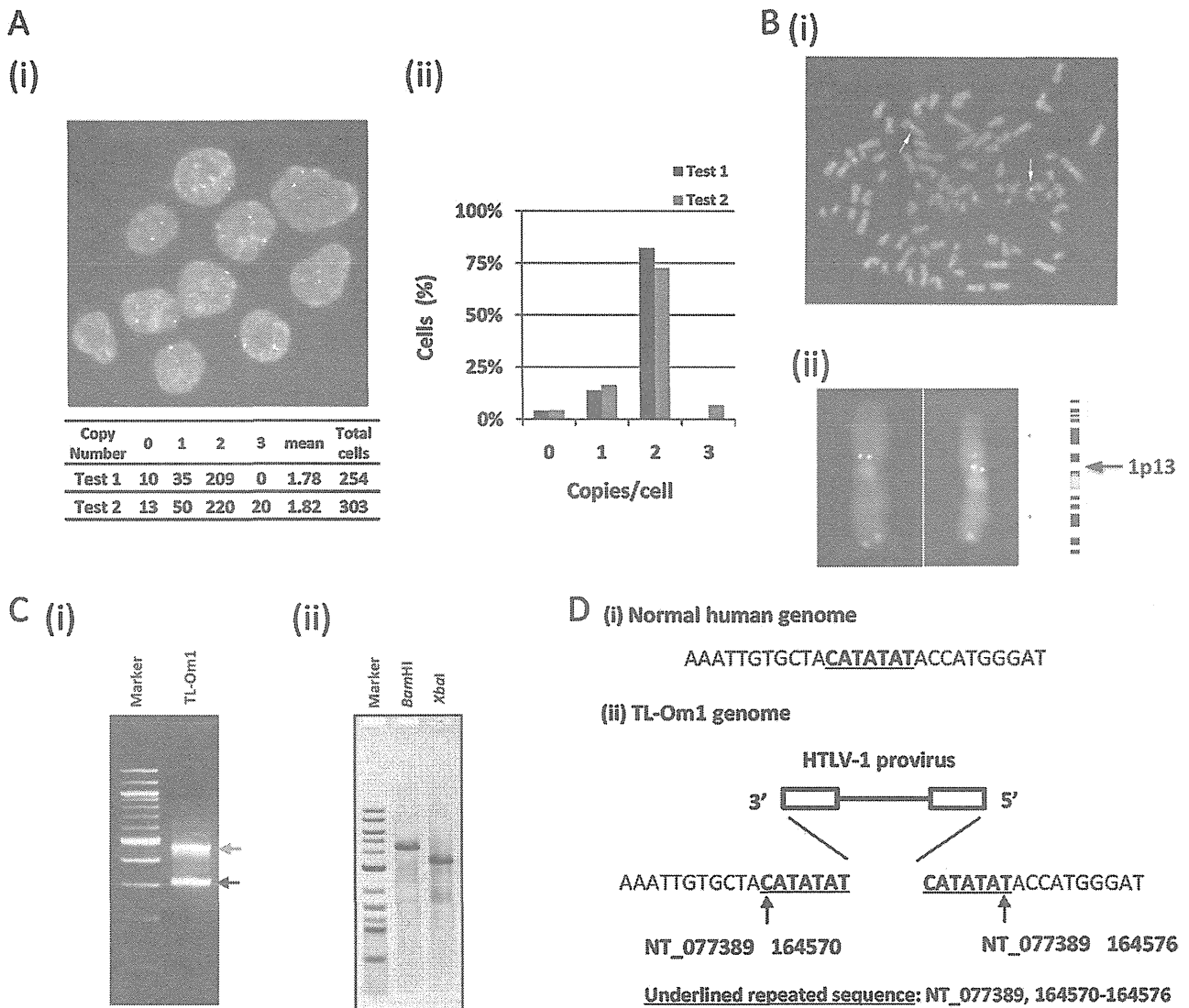


**FIG 2** Clonality, copy number, and integration site of HTLV-1 in TL-Om1 cells. (A) HTLV-1 proviral copy number per cell was determined by FISH using an HTLV-1 full-genome probe. (i) Yellow signals indicate the HTLV-1 probe. Lower table shows the counts of HTLV-1 signals per cell. (ii) Vertical axis indicates percentage counts of each fraction in relation to total cells. Data were the results from two independent analyses. (B) Number of HTLV-1 integrated chromosomes was determined in metaphase cells with the HTLV-1 and 1q44 probes. (i, ii) Yellow signals indicate the HTLV-1 probe, and red signals indicate the 1q44 probe. All HTLV-1 signals were located on chromosome 1. HTLV-1 signals on chromosome 1 were positioned at 1p13. (C) Determination of the HTLV-1 integration site in TL-Om1 cells. (i) The 3' integration site was determined by Splinkerette PCR with an HTLV-1-specific primer. PCR products were subjected to agarose gel electrophoresis. (ii) BamHI- or XbaI-digested TL-Om1 genomes were self-ligated and subjected to inverse PCR with an HTLV-1-specific primer set. PCR products were subjected to agarose gel electrophoresis. (D) 5' and 3' HTLV-1 integration sites were determined by a sequencing analysis of DNA fragments from both Splinkerette and inverse PCR. (i) Normal human sequence; (ii) determined HTLV-1 integration site. HTLV-1 was inversely integrated at chromosome 1: NT\_077389, 164570 to 164576.

value of target gene primers from the average  $C_T$  value of RPPH1 primers (Table 1). The correction value was calculated as follows: correction  $C_T$  value = correction factor  $\times$  actual  $C_T$  value. By applying the correction factors, we reduced the limits of error of the  $C_T$  values to 0.1 cycles with normal PBMCs (data not shown).

**Digital PCR analysis.** Primers and probes for digital PCR analysis of HTLV-1 were previously reported (11, 15). In brief, the primers and probe for HTLV-1 were as follows: forward, 5'-CGGATACCCAGTCTACGTGTT-3'; reverse, 5'-CAGTAGGGCGTGACGATGTA-3'; probe, FAM-5'-CTGTGTACAAGGCGACTGGTGCC-3'-TAMRA (where FAM is 6-car-

boxyfluorescein and TAMRA is 6-carboxytetramethylrhodamine). The primers and probe for albumin were as follows: forward, 5'-TGTCATCTCTTGTGGGCTGT-3'; reverse, 5'-GGTTCTCTTTCACGTGACATC TGC-3'; probe, FAM-5'-CCTGTCATGCCACACAAATCTCTCC-3'-TAMRA. The mixture of primers and probe for RPPH1 was purchased from Applied Biosystems. The PCR mixture was prepared using 2 $\times$  digital droplet PCR (ddPCR) supermix for probes (Bio-Rad, Hercules, CA, USA). Droplets were prepared on a QX100 droplet generator (Bio-Rad). PCR was performed with a LifePro thermal cycler (Bio-Rad) and detected with a QX100 droplet reader (Bio-Rad). Data were means of triplicate analysis.



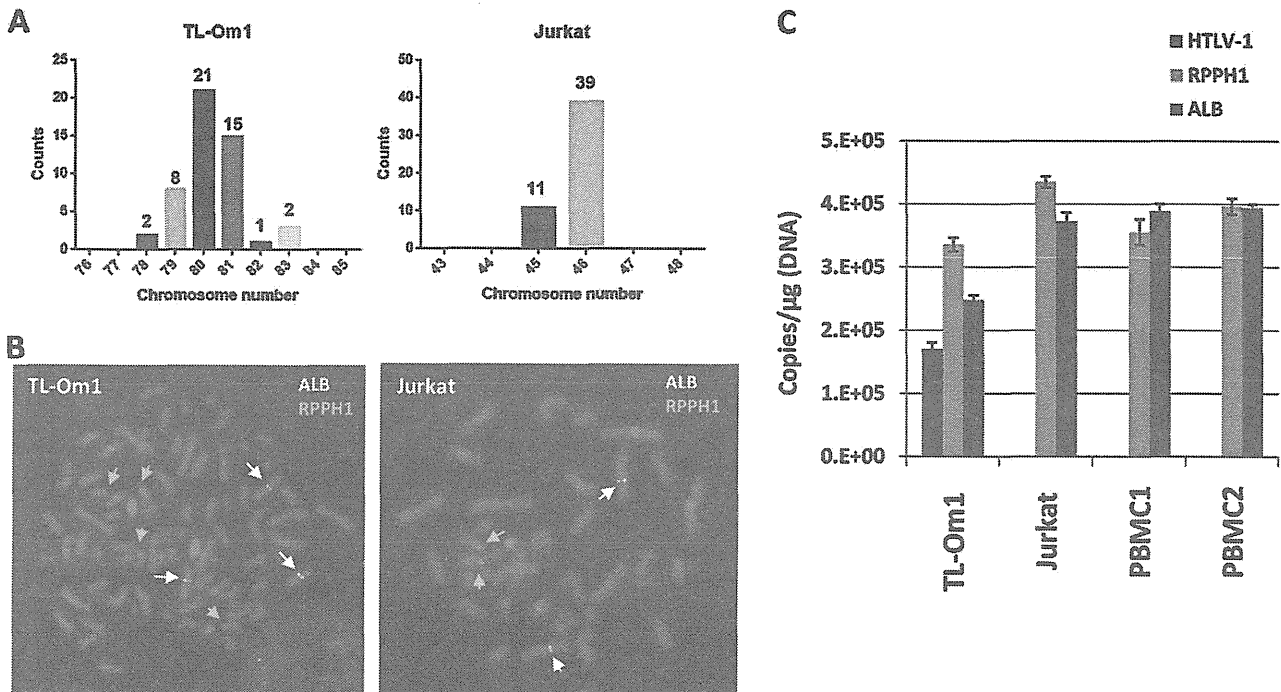


**FIG 3** Gene copy number of IC cellular genes for HTLV-1 qPCR. (A) The number of chromosomes in TL-Om1 and Jurkat cells at metaphase was counted. Horizontal line indicates the number of chromosomes per cell. (B) Representative FISH images of TL-Om1 and Jurkat cells at metaphase. Yellow and red arrows indicate signals for ALB and RPPH1 probes, respectively. Left panel shows three signals for ALB and four for RPPH1; right panel shows two signals for ALB and two for RPPH1. (C) Determination of the gene copy number of HTLV-1, RPPH1, and ALB genes by digital PCR. gDNA of TL-Om1 and Jurkat cells and of PBMCs from two healthy donors were subjected to digital PCR. Data show the absolute copy number of HTLV-1, RPPH1, and ALB genes per microgram of gDNA. Bars are means from triplicate analyses.

**In vitro HTLV-1 infectivity test.** Frozen cells were thawed and immediately cultured for a week. Exponentially growing cells were used for the assay. Jurkat, TL-Om1, SLB1, and HUT102 cells were treated with 50 µg/ml mitomycin C (Kyowa Hakko Kirin, Tokyo, Japan) and incubated for 1 h at 37°C. After being washed twice with 2% FBS-PBS,  $1 \times 10^5$  cells were added to culture medium containing  $1 \times 10^6$  Jurkat cells. Mitomycin C was used to block the growth of ATL cell lines added to Jurkat cells. Cells were cocultured for 2 weeks and then subjected to qPCR to determine PVL, as described previously (11).

**RESULTS**

**HTLV-1 infectivity in TL-Om1 cells.** We investigated the production potential of infective virus to ascertain the clonal stability of HTLV-1 integration *in vitro*. Mitomycin C-treated TL-Om1 cells were cocultured with Jurkat cells for 2 weeks. At the end of the 2 weeks, no HTLV-1 integration was observed in the Jurkat cells that were cocultured with TL-Om1 cells, while HTLV-1 integration was observed when Jurkat cells were similarly cocultured with SLB-1 and HUT102 cells (Fig. 1A). These findings suggested that the production of infective HTLV-1 particles from TL-Om1 cells was low or diminished; thus, the increase in copy number over the course of cell culture was thought to be negligible. If TL-Om1 cells had infectious potential, the clonality of HTLV-1 provirus in them would vary because of the mutual HTLV-1 infections between cells. To evaluate the clonality of HTLV-1 provirus in TL-Om1 cells, TL-Om1 gDNA was analyzed by Southern blotting. EcoRI-digested gDNA showed a single band, while PstI digestion produced five DNA bands that contained an HTLV-1 sequence

(Fig. 1B). Three of the five DNA bands were HTLV-1 internal sequences. The other two DNA bands contained either 5' or 3' HTLV-1 sequences ligated with the host genome (Fig. 1B). These fragment patterns indicated that HTLV-1 provirus integration in TL-Om1 cells was monoclonal.

**Determination of copy number and integration site of HTLV-1 provirus by FISH.** To confirm the clonality and copy number of HTLV-1 provirus and of IC genes in detail, we performed a FISH analysis. There were one or two signals of HTLV-1 provirus in the cells. The mean proviral copy number was calculated at 1.8 copies/cell from the count of signals with >250 cells in two independent analyses (Fig. 2Ai and ii). Double-staining of the TL-Om1 genome with both HTLV-1 and 1q44 probes in meta-

**TABLE 2** Gene copy number of IC genes determined by FISH

Karyotype	Gene copy no.			
	TL-Om1 (20 analyzed cells)		Jurkat (20 analyzed cells)	
	RPPH1 gene	ALB gene	RPPH1 gene	ALB gene
2N	0	0	20	20
3N	1	20	0	0
4N	19	0	0	0
Average	3.95	3	2	2
Ratio to the RPPH1 gene	1	0.76	1	1

TABLE 3 Summary of ratio of gene copy numbers to the RPPH1 gene

Method	Cell line	Gene copy no. ratio to the RPPH1 gene							
		RPPH1 gene	ALB gene	ACTB gene	CD81 gene	HBB gene	RAG-1 gene	HTLV-1 gene	LTR gene
FISH	TL-Om1	1.00	0.76					0.46	
	Jurkat	1.00	1.00						
Digital PCR	TL-Om1	1.00	0.74					0.51	
	Jurkat	1.00	0.86						
	PBMC1	1.00	1.09						
	PBMC2	1.00	0.99						
qPCR (plasmid)	TL-Om1	1.00	0.74					0.48	1.02
	Jurkat	1.00	0.92						
qPCR (gDNA)	TL-Om1	1.00	0.74	1.18	0.99	0.92	0.94		
	Jurkat	1.00	0.95	1.07	0.99	0.90	1.08		
	PBMC 1	1.00	0.99	1.00	0.98	0.99	1.00		
	PBMC 2	1.00	1.01	1.01	0.99	1.00	1.01		

phase showed that all HTLV-1 DNA signals were located on chromosome 1 (Fig. 2Bi). When the number of copies of chromosome 1 was 1, 2, 3, or 4 per cell, the number of HTLV-1 proviruses per cell was 1, 1, 2, and 2, respectively (data not shown). HTLV-1 signals on chromosome 1 were positioned on the band of 1p13 (Fig. 2Bii). These results correlated well with the Southern blotting results that showed monoclonal integration.

#### Confirmation of integration site of HTLV-1 in TL-Om1 cells.

To identify the integration site of monoclonal HTLV-1 provirus, Splinkerette PCR was performed with TL-Om1 gDNA. Two specific PCR products were obtained by gel electrophoresis (Fig. 2Ci). The DNA fragments were analyzed by direct sequencing. Sequencing analysis of the lower-molecular-weight DNA fragments (Fig. 2Ci, lower band) showed that they were provirus genomic sequences. Sequencing analysis of the higher-molecular-weight band showed that it contained host gDNA ligated to the 3' LTR of HTLV-1. We also performed inverse PCR with TL-Om1 gDNA that was digested with BamHI or XbaI followed by self-ligation. Single DNA bands were obtained from both BamHI and XbaI self-ligated templates (Fig. 2Cii). Sequencing analysis demonstrated that both bands contained the same sequences. A BLAST search revealed that the sequence was located on chromosome 1. The integration site was identified, and the HTLV-1 provirus was integrated inversely in between the CATATAT repetitive sequences at the region of NT\_077389 from nucleotides (nt) 164570 to 164576 on chromosome 1 (Fig. 2Di and ii).

We determined the full-length sequence of HTLV-1 provirus in TL-Om1 cells by genomic long PCR followed by direct sequencing. The length of HTLV-1 provirus was determined to be 8,941 bp (GenBank accession no. AB979451; see also Text S1 in the supplemental material). The percent identity to the HTLV-1 genomic sequence of the ATK-1 strain (accession no. J02029) was 98.7%. Compared with the full-length HTLV-1 genomic sequence of ATK-1, there was a 93-nt deletion in the *env* gene. The region that was deleted was equivalent to nt 5547 to 5669 of ATK-1. The deduced amino acid sequence of the deletion was 31 in-frame amino acids ( $\Delta$ 125–155 of Env). The deleted region was located on the receptor binding domain of Env (see Fig. S1 in the supplemental material).

#### Calculation of chromosome and gene copy numbers of HTLV-1, RPPH1, and ALB genes in TL-Om1 and Jurkat cells.

We counted the chromosome number in TL-Om1 and Jurkat cells by FISH analysis. Jurkat cells were analyzed as one of the control cell lines. The chromosome number differed from 78 to 83 in TL-Om1 cells (Fig. 3A). The mean chromosome number was estimated at 80.2, which indicated that the karyotype of TL-Om1 cells was about 4N. There were 45 or 46 chromosomes in Jurkat cells, indicating that their karyotype is near that of normal human diploid cells (Fig. 3A and B and Table 2).

The absolute gene copy number of HTLV-1 provirus and IC genes was measured using digital PCR. gDNA from TL-Om1 cells, Jurkat cells, and PBMCs from two healthy donors was subjected to digital PCR and used to calculate the copy numbers of these genes (Fig. 3C). Although the ALB-to-RPPH1 gene copy number ratios in the two PBMC samples were 1.09 and 0.99, the ALB-to-RPPH1 gene copy number ratio in TL-Om1 cells was low (ratio of 0.74) (Table 3). The provirus-to-RPPH1 gene copy number ratio in TL-Om1 cells was 0.51 (Table 3). These results were consistent with the provirus- and ALB-to-RPPH1 gene copy number ratios estimated by FISH, which were 0.46 and 0.76, respectively (Table 3). The usefulness of TL-Om1 as a reference standard is strongly supported by the consistent results from the FISH and digital PCR analyses (Table 4).

**Estimation of the gene copy number of HTLV-1 and IC genes by synchronized qPCR.** We previously developed a method to determine inherited allelic deletions by using qPCR with primer sets that can amplify fragments synchronously, even though the

TABLE 4 Absolute gene copy number per microgram gDNA determined by digital PCR

Cell line	Gene copy no./ $\mu$ g gDNA <sup>a</sup>		
	HTLV-1 gene	RPPH1 gene	ALB gene
TL-Om1	170,171.1	335,452.3	248,410.8
Jurkat	NT	434,529.6	373,423.9
PBMC1	NT	355,116.1	388,650.0
PBMC2	NT	397,260.3	394,520.5

<sup>a</sup> Data are means of triplicate analysis. NT, not tested.

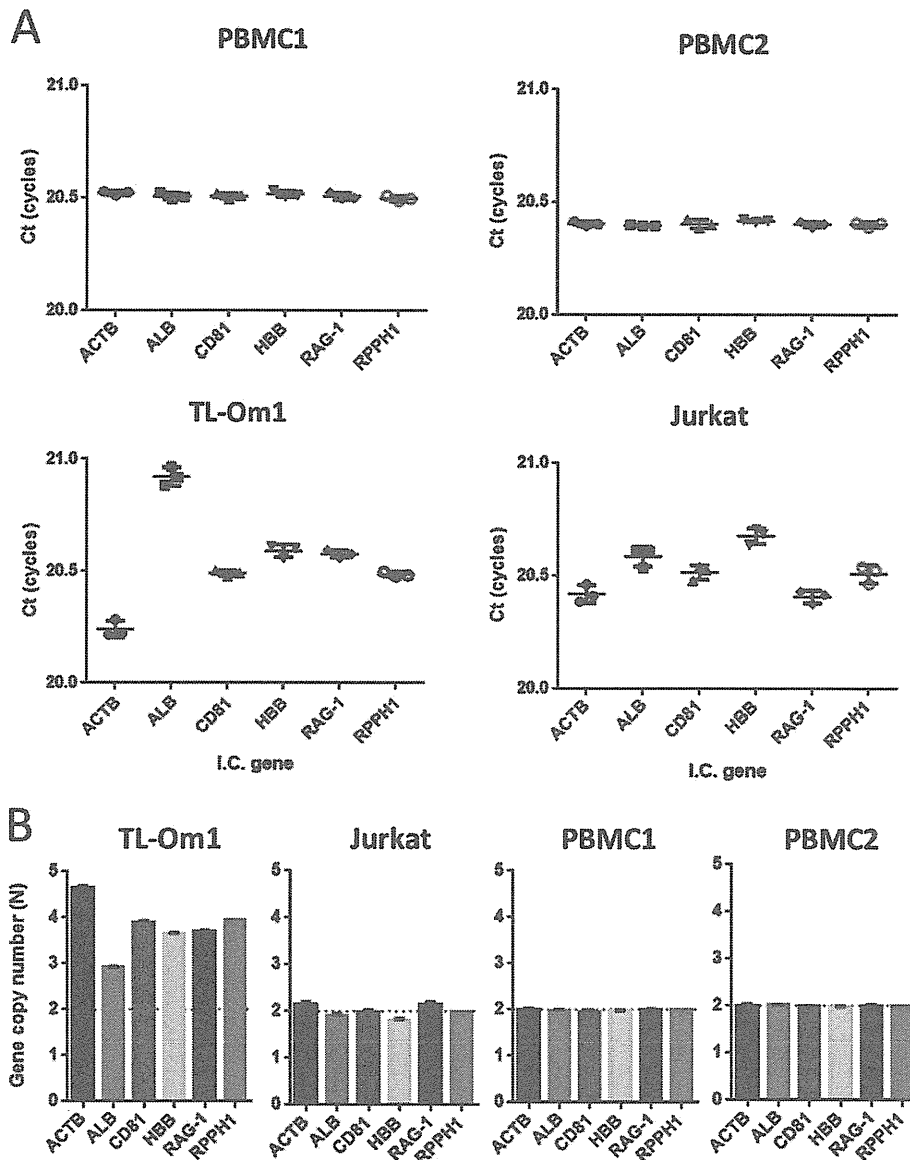


**FIG 4** Estimation of gene copy number of IC genes in TL-Om1 cells by qPCR. gDNA of TL-Om1 and Jurkat cells and of PBMCs from two healthy donors was tested by qPCR with synchronous amplification primer sets for IC genes. (A)  $C_T$  scores (cycles) of each primer set for IC genes. Each dot indicates the mean from triplicate analyses. The  $C_T$  scores in the graph were the results of correction by the factors described in Table 1. (B) Estimated gene copy number of IC genes calculated using the difference in  $C_T$  scores from RPPH1. The copy numbers of IC genes of TL-Om1 and Jurkat cells were calculated based on FISH analysis for the RPPH1 gene. RPPH1 gene copy number from PBMCs was set as 2N. Equation for the estimation of gene copy number was as follows: gene copy number (N) = RPPH1 gene copy number determined by FISH analysis  $\times 2^{-\Delta C_T}$ ,  $\Delta C_T = C_T(\text{target gene}) - C_T(\text{RPPH1})$ .

target genes are different. The method shows that the difference in  $C_T$  value determines the difference in gene copy number. We used primer sets for HTLV-1 genes (LTR and coding regions) and ACTB, ALB, CD81, HBB, and RAG-1 IC genes (Table 1). To increase the specificity, we used primer correction factors, which compensate for the slight difference in PCR amplification efficiency between different primers for target genes. As shown in Fig. 4A, TL-Om1 and Jurkat cells did not show the complete synchronized amplifications that were observed in normal PBMCs. By setting the PCR amplification efficiency of all primer sets per cycle

to approximately 2-fold, the ratio of the gene copy number against the RPPH1 gene was estimated using the difference in the mean  $C_T$  scores of the IC gene primer sets from the mean of those for the RPPH1 gene. The ratios of the gene copy number of the ALB gene to that of the RPPH1 gene in TL-Om1 and Jurkat cells were 0.74 and 0.92, respectively (Table 3). When the copy number of the RPPH1 gene in TL-Om1 cells was set at 3.95, which was determined by FISH analysis, the copy number of the IC genes was at least 2.9 (ALB gene) and at most 4.7 (ACTB gene) (Fig. 4B and Table 3).

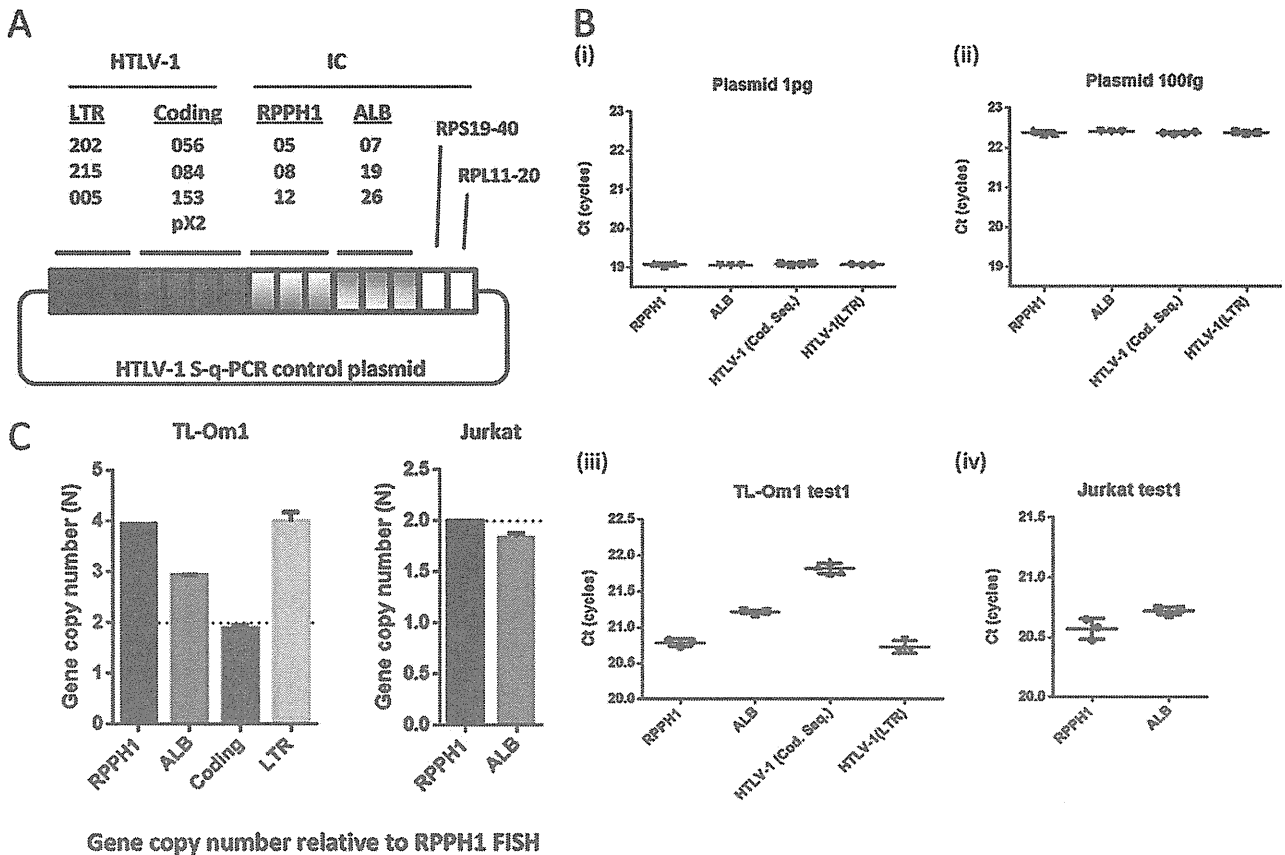


**FIG 5** Estimation of the HTLV-1 gene copy number in TL-Om1 cells by synchronized qPCR. gDNA of TL-Om1 and Jurkat cells and of PBMCs from two healthy donors was tested for qPCR with synchronous amplification primer sets for HTLV-1, RPPH1, and ALB genes. (A) Construction of control plasmid with a single copy of each target sequence; (B) data indicate  $C_T$  scores of HTLV-1, RPPH1, and ALB genes for control plasmid at 1 pg, 100 fg/reaction, and for TL-Om1 and Jurkat cells. qPCR with the plasmid showed synchronous amplification of all primer sets. Each dot indicates the mean from triplicate analyses. The  $C_T$  scores in the graph are the results of correction by the factors described in Table 1. (C) Estimated HTLV-1 and ALB gene copy number in TL-Om1 and Jurkat cells. Data were estimated using the difference in  $C_T$  scores between target genes and RPPH1 genes.

Additionally, we tried to determine the HTLV-1 copy number in TL-Om1 cells using a synchronized qPCR method. We prepared a plasmid that had one copy of every target PCR amplicon (Fig. 5A). The plasmid had the same copy number as all the target regions. Using the plasmid as a template, we performed qPCR and confirmed the synchronized amplification of primer sets for HTLV-1, RPPH1, and ALB genes (Fig. 5B). The difference in mean  $C_T$  scores for the HTLV-1 gene to the RPPH1 gene was 1.05 cycles on average in TL-Om1 cells (Fig. 5C and Table 3). As with the sequencing analysis, use of the synchronized qPCR method also estimated the copy number of the LTR to be 4.01, indicating that TL-Om1 cells have two LTRs (Fig. 5C and Table 3).

**Comparison of HTLV-1 copy number from different calculation methods.** We compared the results of HTLV-1 and ALB gene copy number obtained from FISH, digital PCR, and synchronized qPCR. The copy number ratios of the HTLV-1 gene to the RPPH1 gene in TL-Om1 cells were 0.46, 0.51, and 0.48, from FISH, digital PCR, and synchronized qPCR, respectively, and those for the ALB gene were 0.76, 0.74, and 0.74 (Fig. 6 and Table 3). The results from these varied assays strongly support one another, indicating that TL-Om1 cells are suitable for use as a reference material for HTLV-1 qPCR.

## DISCUSSION

Recently, NAT reference materials have been established for the safety of blood and blood products, such as international standards for HIV, hepatitis B virus, and hepatitis C virus (22–24). These materials have been frequently used for the purpose of calibration and validation of test systems, preparation of secondary reference materials, and comparison of multicenter results, which have helped improve the consistency of the results. Most international standards for blood-transmitted viruses use plasma from infected human blood, because the test target is extracted from human plasma. With regard to HTLV-1 NAT, it may be better to use a cell line as a reference material to standardize the qPCR results, because this test uses cells obtained from peripheral blood. An example of NAT reference material using cell lines is reported in a test for quantitation of BCR-ABL mRNA. Panels of K562 cells combined with HL60 cells were set as standards, which have been approved by the WHO Expert Committee of Biological Standardization (25). Although a variety of cell lines harboring HTLV-1 provirus in their genomes has been established, detailed characterization of the candidate cell lines with regard to their suitability as reference materials for HTLV-1 NATs has not yet been per-